Effect of wire material and discharge energy on productivity and surface integrity of WEDM-processed Inconel 718

Abhilash P. M.*, D. Chakradhar

Department of Mechanical Engineering, Indian Institute of Technology Palakkad, Kerala, India, 678557

*Corresponding author: abhilashpm184@gmail.com, ORCID ID: 0000-0001-5655-6196

Abstract: The current work aims to study the influence of discharge energy and debris accumulation on wire break failure and surface integrity aspects like surface roughness, subsurface hardness, and geometrical errors during the wire EDM of Inconel 718. The responses considered for analyzing the geometrical accuracies are flatness error, roundness error and cylindricity error. Four different wire electrodes were considered for the study based on the wire strength and coatings, namely hard zinc coated brass, half-hard zinc coated brass, hard uncoated brass, and half-hard uncoated brass wire electrodes. The geometric accuracy of the machined parts is closely related to the choice of wire electrode. High tensile strength hard wires were observed to machine the surfaces with maximum accuracy. Also, the zinc coated wires were observed to cut faster compared to the uncoated wire electrodes. The study revealed that there exists a strong influence of discharge energy on the surface integrity of wire electric discharge machined surface. The zinc and copper elemental contamination was minimal for uncoated wire electrodes at lowest discharge energy mode. Wire wear phenomena was analysed for both coated and uncoated wires. Discharge energy had a significant impact on the electrode wear of coated and uncoated wire electrode.

Keywords: WEDM, discharge energy, geometric accuracy, surface integrity, wire wear, coated electrode, Inconel 718

1. Introduction

Superalloys are the class of materials which has unique high temperature properties. They normally find their applications in turbine, nuclear, aerospace industries etc. The ability to perform at temperatures closer to the melting point makes them suitable for such applications. Super alloys are observed to exhibit creep, fatigue and corrosion resistance apart from their high strength and hardness. It is estimated that more than half of the components in gas turbine are made of Ni based superalloys. Since it is employed in the hottest of the turbine sections, utmost importance shall be given to the precision and surface integrity of such machined components [1]. However, machining such superalloys using conventional techniques is rather difficult because of multiple reasons. Work hardening tendency, Built-Up-Edge (BUE) formation, adhesion with cutting tool, low thermal conductivity, high tool wear and presence of hard carbides are some of the reasons why the superalloys are classified "difficult-to-machine".

Wire electric discharge machining is a suitable alternative to machine nickel-based superalloys due to its non-contact nature of material removal [2]. The material removal mechanism involves controlled spark erosion through a programmed contour. The non-contact nature of material removal enables the machining of superalloys, titanium alloys, cemented carbides, conductive ceramics etc. Even though the machining efficiency is less, the surface finish and accuracy are very high. A direct analytical equation for responses does not exist for wire EDM process due to its stochastic nature. Also, the productivity and quality related responses are material dependent and have to be experimentally analysed separately for developing response models [3]. In this regard, parametric study and optimization of WEDM process for different work materials have been attempted by many researchers in the past [4-6].

Discharge energy could be considered as one of the most critical parameters in wire electric discharge machining. However, only limited works are reported on its effect on the WEDM responses. Li et al. [7] studied the effect of discharge energy on the surface integrity during the

WEDM of Inconel 718. Surface roughness, surface contamination and white layer thickness were observed to be minimum for lower discharge energy. Sharma et al. [8] observed that the cutting rate, recast layer, surface roughness and residual stresses increased with increase in discharge energy. Cabanes et al. [9] observed that the machining instability and wire breakages are dependent on discharge energy. A condition monitoring system was developed which triggers different alarms based on the severity of instability. Kumar et al. [10] studied the surface topography and morphology for different discharge energies during wire electric discharge machining of Nimonic 90 superalloy. Caggiano et al. [11] developed an algorithm to classify pulse types into normal sparks and abnormal sparks. Short circuit sparks were observed to cause surface damages and wire breakages.

Profile accuracy related parametric study for WEDM process is attempted by a few researchers in the past. Straka et al. [12] modelled profile accuracy of machined surface by considering flatness error as the response. The wire vibration was observed to be a major contributor for geometric inaccuracy. Abyar et al. [13] studied the corner profile errors during wire EDM finish passes. Prohaszka et al. [14] had observed that the wire oscillation is greatly related to the machined surface accuracy. Islam et al. [15] used traditional analysis, pareto ANOVA and Taguchi method to perform parametric study on the dimensional and geometric accuracies of machined parts. Kumanan and Nair [16] performed multi objective optimization of performance characteristics like cylindricity, roundness, parallelism and perpendicularity using grey ANFIS. Senkathir et al. [17] optimized the wire EDM parameters using RSM. The responses considered were circularity, material removal rate and surface roughness. Pramanik et al. [18] observed that the profile inaccuracy is dependent on heat generation, heat dissipation and debris removal from the machining zone.

Ramamurthy et al. [19] performed performance comparison of various wire electrodes during the wire-EDM of Ti-6Al-4V. Reolon et al. [20] compared the effect of wire coatings on machining performance and surface integrity of the machined surface and coated wire was found to perform better. Jadam et al. [21] observed a reduction in recast layer thickness and kerf width while using coated wires compared to that of uncoated wire electrodes. Klocke et al. [22] explored the improvement of cutting rates while using coated wires. The Ni coated wire electrodes were observed to provide the maximum cutting rate. However, a better accuracy was observed using standard brass wire. The machining is said to be unstable in the following conditions: poor flushing due to lack of dielectric (due to lesser than optimum spark gap), lesser time between discharges causing inefficient debris removal and cooling (due to small pulse off time), and excessive discharge energy producing a greater amount of debris [23].

The modern aerospace industries, especially gas turbine industries, prioritizes two aspects of machined components: (a) surface integrity, and (b) geometrical accuracy [22, 24, 25]. Inconel 718 is a well-known and widely used material for manufacturing gas turbine parts. It is therefore industrially relevant to explore ways to improve the above mentioned two aspects during the machining of Inconel 718 superalloy. Improperly machined component with considerable geometrical errors can eventually lead to component failure due to wear, vibrations, heat generation etc. Even after the manufacturing processes have become smarter and advanced, the geometrical errors are yet to be eradicated completely. Also, the EDMed superalloys are still not considered extensively for high temperature applications because of its inferior surface integrity [25]. The previous studies that dealt with surface integrity of machined components haven't considered the geometrical accuracy aspects [7, 8]. Also, the earlier studies on geometrical accuracies haven't considered the effect of wire electrode material and wire tensile strength [12, 15-17].

The literature review indicates that the major research focus in wire electric discharge machining of superalloys are on studying the influence of process parameters on the performance characteristics. However effect of wire electrode and machining stability on geometric accuracy of wire EDMed parts are yet to be discussed. In this context, the current experimental study aims to investigate on the effect of wire electrode materials and discharge energy on geometric accuracy and surface integrity of WED machined Inconel 718 surfaces. Since a the wire wear mechanism during wire EDM is also yet to be analysed, the present study also investigates the extend of wire wear for coated and uncoated wire electrode surfaces. Thus, the experimental analysis is expected to take the process a step closer to gas turbine industries' demands of tight geometric tolerances and excellent surface integrity.

2. Materials and Methods

2.1 Material Selection

Inconel 718 is chosen as the work material for the current experimental study due to its industrial significance. The thickness of work material is 10 mm. The profile to be machined is shown in Fig. 1. Such a profile is selected because it contains all the geometric features to measure the various form errors considered in this study. The chemical and mechanical properties of Inconel 718 are given in Table 1 and Table 2 respectively. Three types of wire electrodes are chosen for this study namely 'hard', 'half-hard' and 'soft' based on their capacity to withstand the testing conditions in the inter electrode gap. The tensile strengths of the 'hard', 'half-hard' and 'soft' types are 900 MPa, 490 MPa and 440 MPa respectively.

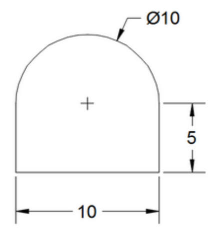

Fig. 1. Profile of the part machined (All dimensions in mm)

Table 1. Chemical Composition of Inconel 718 [1]

Element	**Ni**	**Fe**	**Cr**	**Nb**	**C**	**Al**	**Ti**	**Mo**
Weight (%)	Balancing	18.5	19	5.1	0.04	0.5	0.9	3

Table 2. Mechanical Properties of Inconel 718

Property	**Value**
Density	8.19 g/cm^3
Melting Point	1260 – 1336°C
Specific Heat	435 J/kg K
Average Coefficient of thermal expansion	13 µm /m K
Thermal Conductivity	11.4 W/m K
Ultimate Tensile strength	1240 MPa

2.3 Experimental Setup and Equipment

Machining was performed on Electronica ECOCUT wire electric discharge machine. ELCAM software was used to program the machined profile. The machine axis is servo controlled with 1 µm resolution. Wire electrodes with 0.25 mm diameter were selected. Deionized water with a conductivity ~20 µS/cm is taken as the dielectric medium. Form errors were measured by Accurate Tutor 5.5.4 coordinate measuring machine (CMM). Zeiss Surfcom Flex 35-B contact type surface profilometer was used to measure the surface roughness. Field emission scanning electron microscope (FESEM) - Zeiss GeminiSEM 300 was used to image the machined samples and wire electrodes. A non-contact surface profilometer AEP Nanomap1000 WLI was used to image 3D surface morphology. Subsurface microhardness studies were conducted using Wilson VH1102 microhardness tester. The load applied was 10 kgf for a dwell time of 10s.

For the current study, five discharge energy modes were selected. In the past researchers have introduced many methodologies to introduce machining instabilities. In this study, debris accumulation is deliberately created by varying four parameters together. Table 3 shows the parameter combinations for each discharge energy modes. The energy modes are labelled as condition 1 (C1) to condition 5 (C5) in the decreasing order of discharge energies. Maximum debris accumulation in condition C1 is achieved by a combination the following factors

- High T_{on} implies, higher discharge energy. This results in high debris production
- Low servo voltage value implies narrow inter electrode gap. Thus it is difficult to flush away debris and result in debris stagnation
- Low T_{off} implies, lesser than ideal time to flush debris away
- Low wire feed rate implies, higher chances of wire degradation

In the subsequent condition, C2 to C5, the debris accumulation is reduced by relaxing the unideal parameter combinations. The parameter settings for condition 1 to 5 are selected using a strategy similar to the one used by Sharma et al. [8] in his experimental work. Also, the authors have previously investigated the effects of machining stability and discharge energy during the machining of Inconel 718 using this similar approach [26]. In earlier studies, authors have confirmed the existence of debris from the pulse cycle diagrams. Short circuit and arc discharges were present at unstable conditions. Pilot experiments were also conducted to ensure that the process stability is maintained without wire breakages or gap shorts. Table 4 shows the parameter settings that were maintained as constant.

Table 3. Process parameter combinations for different discharge energy levels

Discharge Energy	Symbol	T_{on} (µs)	T_{off} (µs)	Servo voltage (V)	Wire feed (m/min)
Highest (0.01531 J)	C1	116	42	40	3
High (0.01492 J)	C2	113	44	45	5
Medium (0.01452 J)	C3	110	46	50	7
Low (0.01413 J)	C4	107	48	55	9
Lowest (0.01373 J)	C5	104	50	60	11

Table 4. Constant machining parameters

Parameter	Value
Wire electrode diameter	0.25 mm
Discharge current	11 A
Discharge voltage	12 V
Flushing pressure	1.96 bar
Wire Tension	10 N
Dielectric fluid	Deionized water

2.4 Discharge energy of wire EDM

Theoretical discharge energy is given as the product of discharge current, voltage and discharge duration. Theoretical discharge energy calculation is as follows [27]:

$$E_e = \int_0^{t_e} v_e(t).i_e(t).dt \cong V_e.I_e.t_e \quad (1)$$

$$P = V_e.I_e \quad (2)$$

$$E_e \cong P.t_e \quad (3)$$

Where E_e is the theoretical discharge energy, V_e is the discharge voltage, I_e is the discharge current, t_e is the pulse on time and P is power. The discharge current and voltage are kept constant throughout the experimental study. Therefore, the only parameter that cause a change in discharge energy is 'pulse on time'. However, the actual energy of discharge would be different because of the energy loses caused by various factors, many of which are random in nature and difficult to calculate as observed by Li et al. [2]. The parameters like pulse off time, servo voltage and wire feed which have an influence on the actual discharge energy were taken into consideration in the present study. As the pulse off time increases, the spark frequency is less which decreases the discharge energy. Also, at larger servo voltages, the inter electrode gap is large and the intensity of spark reaching the workpiece is lesser. This in turn reduces the discharge energy. Finally, the wire feed rate is observed to have a positive effect on the flushability during the process. Higher the wire feed rate, better is the flushability. [5].

For the current experimental study, since the voltage and current are maintained at 12 V and 11 A respectively, discharge energy per spark is calculated according to equations (2) and (3)

$$\text{Power } (P) = V_e . I_e = 12 \text{ V x } 11 \text{ A} = 132 \text{ W}$$

$$E_e \cong P . t_e = (132\ x\ t_e)\ J \quad (4)$$

The discharge energy per spark for the five different energy modes considered for the study is calculated using equation (4).

2.5 Geometrical errors

Various form errors of machined parts are measured with coordinate measuring machine (CMM). The CMM was calibrated initially by a 30 mm reference sphere to take care of stylus errors. Also, the experimental runs and measurements are repeated and average value is considered to eliminate experimental errors. Geometric errors are associated with the ability of wire electrode to machine in stable condition without wire lags or wire vibrations. Accuracy of the machined profile is therefore directly associated with the wire deflection during machining. In an ideal scenario, the wire is expected to remain vertically straight and follow the programmed path to produce parts with zero deviations from the required profile. This is possible only if there are no forces acting on the wire except the optimum wire tension provided axially to maintain the wire vertically straight. However, during the actual machining, the wire will encounter numerous forces, many of which are stochastic in nature, in the lateral directions as well. These includes the mechanical forces due to the pressure of vapour bubbles caused during sparking, hydraulic forces by the deionized water flushed from top and bottom nozzles, forces due to spark generation etc. [2]. These forces can affect the geometrical accuracy in two ways, namely, by wire deflection or by wire vibrations.

During WEDM, the forces that cause wire deflection are electric discharge forces, electro-magnetic forces, electro-static forces, and forces due to flushing. The cumulative effects of these forces create a backward push, causing the wire to deflect during straight cuts. The applied wire tension tries to negates these forces; however, such wire lag effect is still considered one of the reasons for profile inaccuracies [28]. The wire thus loses its ideal straight position and is bent due to various forces associated with the cutting mechanism. Due to the effective action of the external forces mentioned above, the wire could also vibrate, the amplitude of which depends on the amount of lateral forces the wire has to cope with [29]. Such vibrations can result in geometric errors in machined profile. The extend of geometric inaccuracy would be proportional to the amplitude of vibration.

3. Results and discussion

Experiments were conducted in ‘one factor at a time’ experiment style having a combination of 5 discharge energy modes and 4 wire electrodes resulting in 20 experimental runs. Fig. 2 (a) shows the image of multiple profiles being cut by wire-EDM machine on Inconel 718. Fig. 2 (b) shows a single machined specimen. Such a profile is chosen because most of the basic geometric errors like circularity, cylindricity, flatness etc. can be analysed.

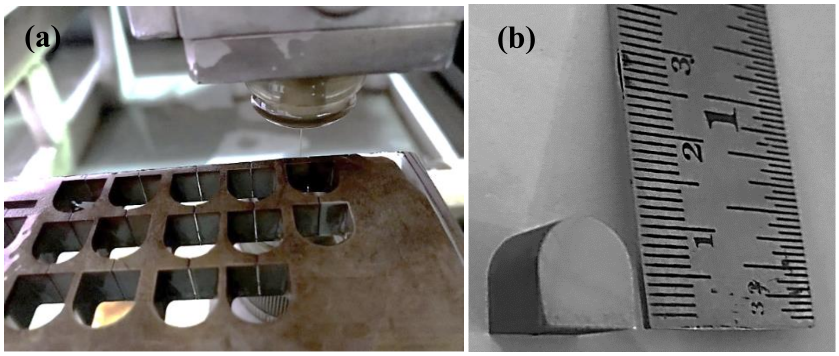

Fig. 2. (a) Multiple slots after a few profiles were cut; (b) A single cut specimen with dimensions

The results of all twenty experimental runs are listed in Table 5. The combinations of all wire materials and discharge energy conditions were considered. Each experiment is repeated thrice and the average value is taken as response. The effect of wire electrode type and discharge energy levels for each response are analysed separately in subsequent sections.

3.1 Cutting speed

Average cutting speed is given by length of travel/machining time. The cutting speed is displayed in the integrated computer of wire EDM. Cutting speed is observed to increase with the discharge energy as evident from Fig. 3 (a). Highest discharge energy (C1) condition resulted in maximum cutting speed. This is because, higher energy sparks will result in larger craters on the workpiece, thus removing greater volume of material per spark. Cumulative effects of such micro crates result in material removal in WEDM process. The end effect is an improvement in the cutting speed as the discharge energy increases. Since the discharge energy is lowest for condition 5 (C5), the cutting speed is also minimal for this energy mode as shown in Fig. 3 (a).

Table 5. Experimental results

Sl. No.	Wire Type	Discharge energy mode	Responses				
			Cutting Speed (mm/min)	Surface Roughness (µm)	Flatness Error (µm)	Circularity Error (µm)	Cylindricity Error (µm)
1	Half-hard uncoated brass	C1	1.20	2.92	3.00	4.20	5.10
2		C2	0.77	2.69	2.90	4.20	4.20
3		C3	0.47	2.42	1.90	1.90	3.20
4		C4	0.44	2.02	1.60	1.80	2.80
5		C5	0.15	1.55	0.50	1.40	2.20
6	Hard uncoated brass	C1	1.25	2.97	2.90	2.40	3.40
7		C2	0.77	2.64	1.10	1.30	3.30
8		C3	0.49	2.14	0.90	0.60	1.80
9		C4	0.47	1.91	0.60	0.80	1.93
10		C5	0.20	1.55	0.51	0.20	1.60
11	Half-hard zinc coated brass	C1	1.55	3.18	3.50	4.70	5.20
12		C2	0.99	2.73	3.20	4.80	4.80
13		C3	0.57	2.49	3.15	4.30	3.40
14		C4	0.49	2.13	1.70	2.50	3.20
15		C5	0.27	1.66	1.30	1.80	2.80
16	Hard zinc coated brass	C1	1.53	3.50	2.95	2.9	3.8
17		C2	1.2	2.93	1.76	2.7	3.48
18		C3	0.62	2.47	1.53	1.7	2.7
19		C4	0.53	2.20	1.2	1.56	1.87
20		C5	0.22	1.73	0.6	0.9	1.9

The cutting speed also varies with the choice of wire electrodes used for machining. Coated wires being able to withstand higher energy sparks resulted in better cutting speeds. The wire could bear such high energies due to the heat sink phenomenon of a lower vapour pressure coating. Also, the rapid melting of zinc coatings increases the instantaneous spark gap resulting in improved flushing conditions. Harder wires resulted in marginally higher cutting speeds. This can be due to the more efficient flushing caused by fewer wire vibrations. Both these effects are evident from the graph shown in Fig 3 (a).

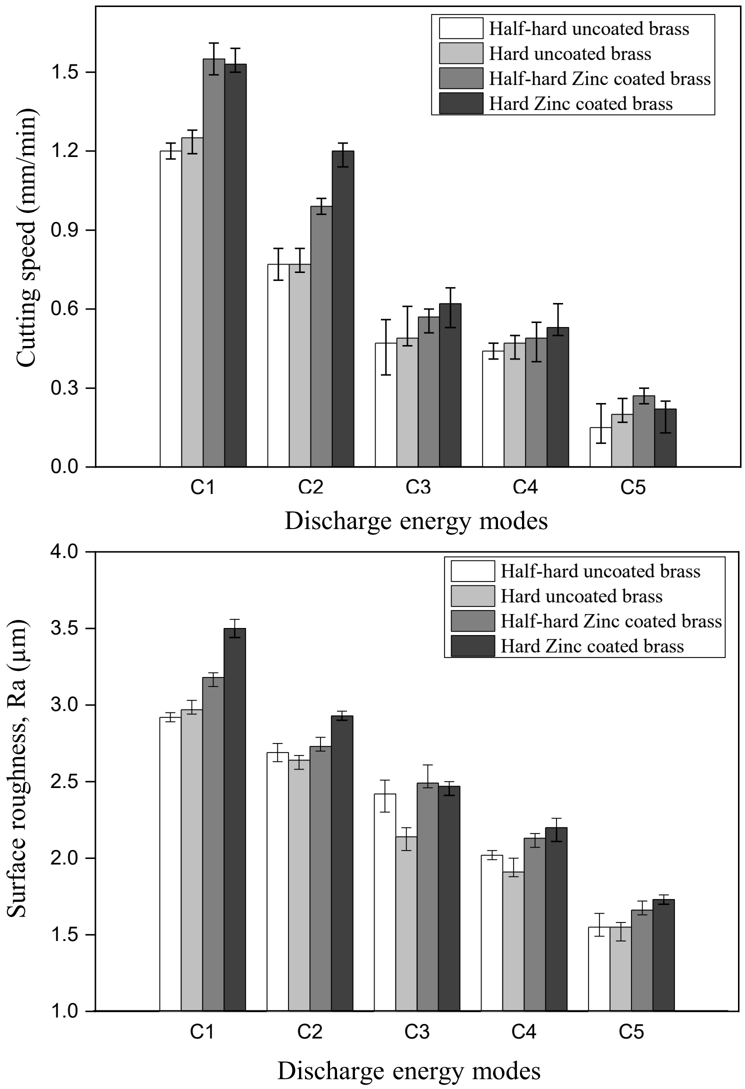

Fig. 3. Effect of wire material and discharge energy on (a) cutting speed (b) surface roughness (R_a)

3.2 Surface roughness

Highest discharge energy mode (C1) resulted in bigger craters per spark. Bigger the crater size, more is the deviation from the mean line, based on which the average surface roughness (R_a) is calculated [30, 34]. Also, at this level, the surface is expected to be coarse in nature with irregular recast layers, micro globules, micro cracks and craters [33]. In contrast, lowest discharge energy mode (C5), resulted in smaller craters, and thus a smoother surface as shown in Fig. 3 (b). R_a value reduced from 3.5 μm (C1) to 1.55 μm (C5). The surface roughness of the surface machined with coated wire electrodes is expected to be higher than the uncoated ones. This is due to higher cutting speed associated with coated wires. However, detrimental effect of coated electrodes on surface finish is partially reduced due to the increase in instantaneous spark gap. This is because of the sudden evaporation of coated zinc from the wire electrode surface. This improves the flushability and thus the wire electrode types did not show any significant effect on the surface roughness

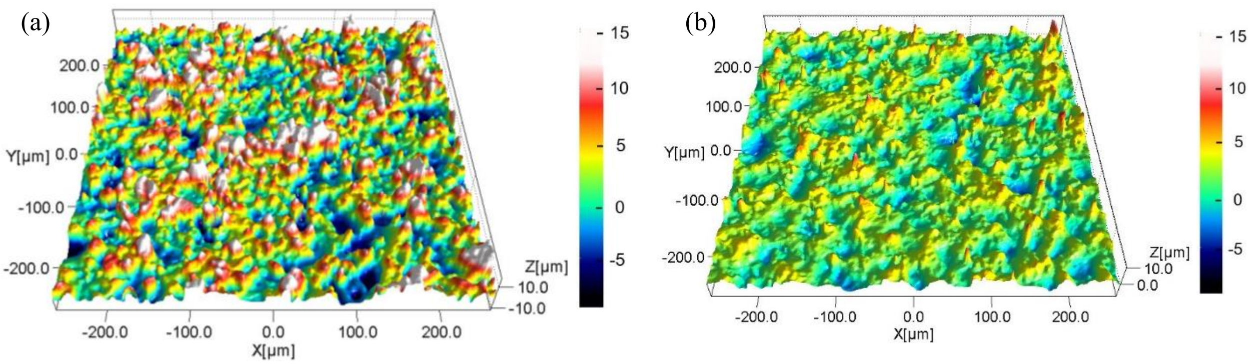

Fig. 4. 3D surface morphology of Inconel 718 machined with hard zinc coated brass electrode at (a) Highest discharge energy, C1 (b) Lowest discharge energy, C5

The machined surface under the conditions C1 and C5, were analyzed using non-contact 3D surface profilometer for the hard zinc coated brass wire electrode. 3D surface morphology images were captured for visual comparison as shown in Fig. 4 (a) and Fig. 4 (b). Similar results were obtained for all other wire electrode types. Clearly due to bigger craters and higher material removal, the surfaces machined at highest discharge energy mode, C1, looks more irregular with steeper peaks and valleys. On the contrary, when machined at condition C5, due to smaller craters and lesser material removal, the surfaces look more levelled with shallower peaks and valleys.

3.3 Geometric errors

Various geometric errors with respect to wire materials and discharge energy is shown in Fig. 5. All the geometric errors were found to be the maximum for condition C1, i.e. the maximum discharge energy setting. The geometrical inaccuracies were found to decrease in the subsequent levels as the machining stability improved, with condition C5 fetching the minimum error. This is because, the amplitude of wire vibration is expected to be dependent on the degree of machining stability. Higher the discharge energy, more intense would be the spark produced and the forces associated with it will be larger. The pressure of vapour bubble produced by a more intense spark would also be higher. Also, the electro-dynamic forces associated with abnormal or harmful sparks are said to be much higher than that from normal sparks. Usually such arc or short circuit pulses are formed from ineffective flushing of debris causing bridging of spark gap. This effect is a common phenomenon at higher discharge energies. The overall effect is higher resultant forces in lateral direction causing higher amplitude wire vibrations. The profile accuracy will improve when machined with reduced discharge energy mode. The most accurate surfaces are produced when machined under discharge energy mode C5, with low energy sparks, larger spark gaps and good enough time to clear debris in between the sparks.

Among different wire electrodes considered, hard wire electrodes were observed to provide better profile accuracies than half-hard wire electrodes. The effect is same for all the geometric errors considered as shown in Fig. 5. This is because hard wires will resist the wire deflections and vibrations better than softer wire electrodes due to their better strength. Also, the uncoated wire electrodes were found to machine with better profile accuracy. This can be due to the marginally better tensile strength of uncoated wires as compared to Zn coated brass wires [8].

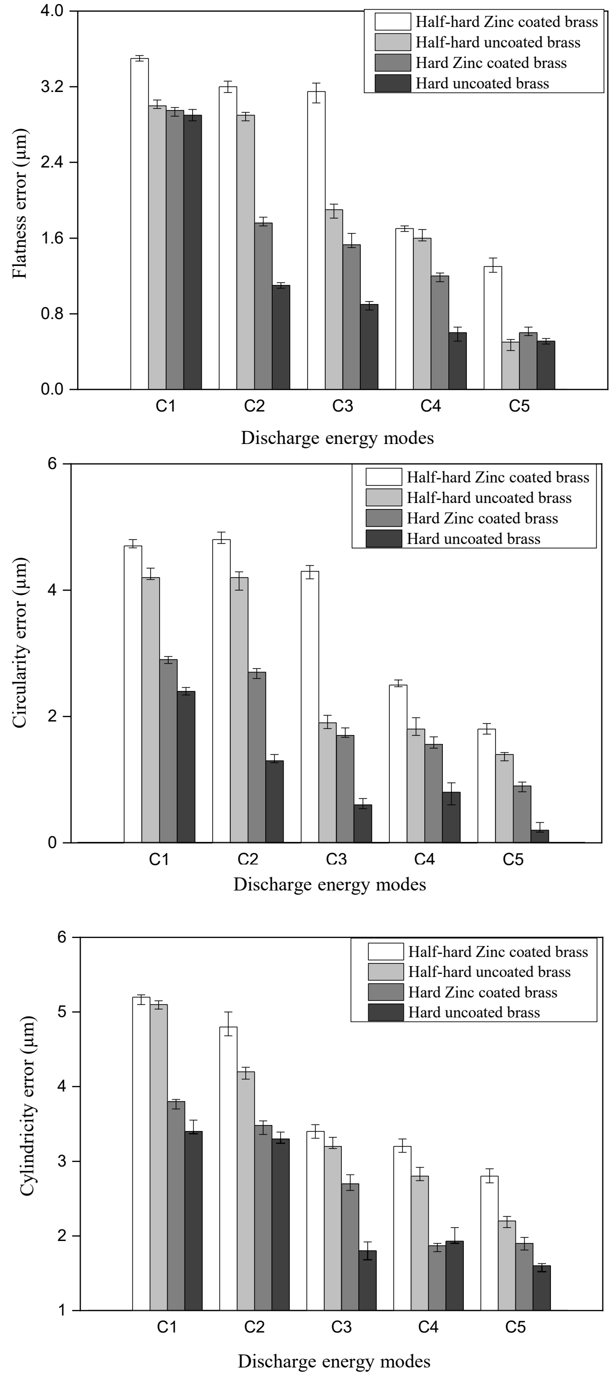

Fig. 5. Effect of wire material and discharge energy on geometrical accuracies (a) Flatness error (b) Circularity error (c) Cylindricity error

3.4 Microstructural analysis of machined surface

Scanning electron microscope (SEM) images were taken and compared for surface morphological changes. Distinct morphological changes could be observed when machined with different discharge energy settings. Fig. 6 shows the SEM images of machined surfaces under different discharge energy modes, when machined with hard zinc coated brass. The wire electrode type didn't have a significant effect on the surface morphology and similar effects were seen for all the wire types considered.

The condition C1 corresponds to the highest discharge energy condition and therefore the machined surface is found to be extremely irregular as evident from Fig. 6 (a). A recast layer formed by re-solidification of molten material is present in the surface, the thickness of which is normally a factor of discharge energy and other process parameters. The irregularity in the surface is due to the presence of micro globules, micro voids, micro cracks and molten debris [31]. At C1, the debris generation is high, spark gap is less and time for flushing is less. This leaves a higher portion of re-solidified material on the machined surface itself.

In the subsequent discharge energy modes, the surface would look more regular with fewer micro globules, however micro voids and porosity can be seen as shown in Fig. 6 (b). Micro voids are formed when vapour gets entrapped in the molten metal which gets re-solidified. Many such surface features together cause the irregularities in the higher discharge energy mode.

The machined surface under discharge energy settings C5 shows almost zero micro cracks, voids, globules or debris deposition. Such a machining condition improves the flushing and produces comparatively lesser amount of debris. The end effect is fewer micro cracks, voids, globules and molten debris. The surface looks the smoothest of all machining conditions considered as evident from Fig. 6 (c)

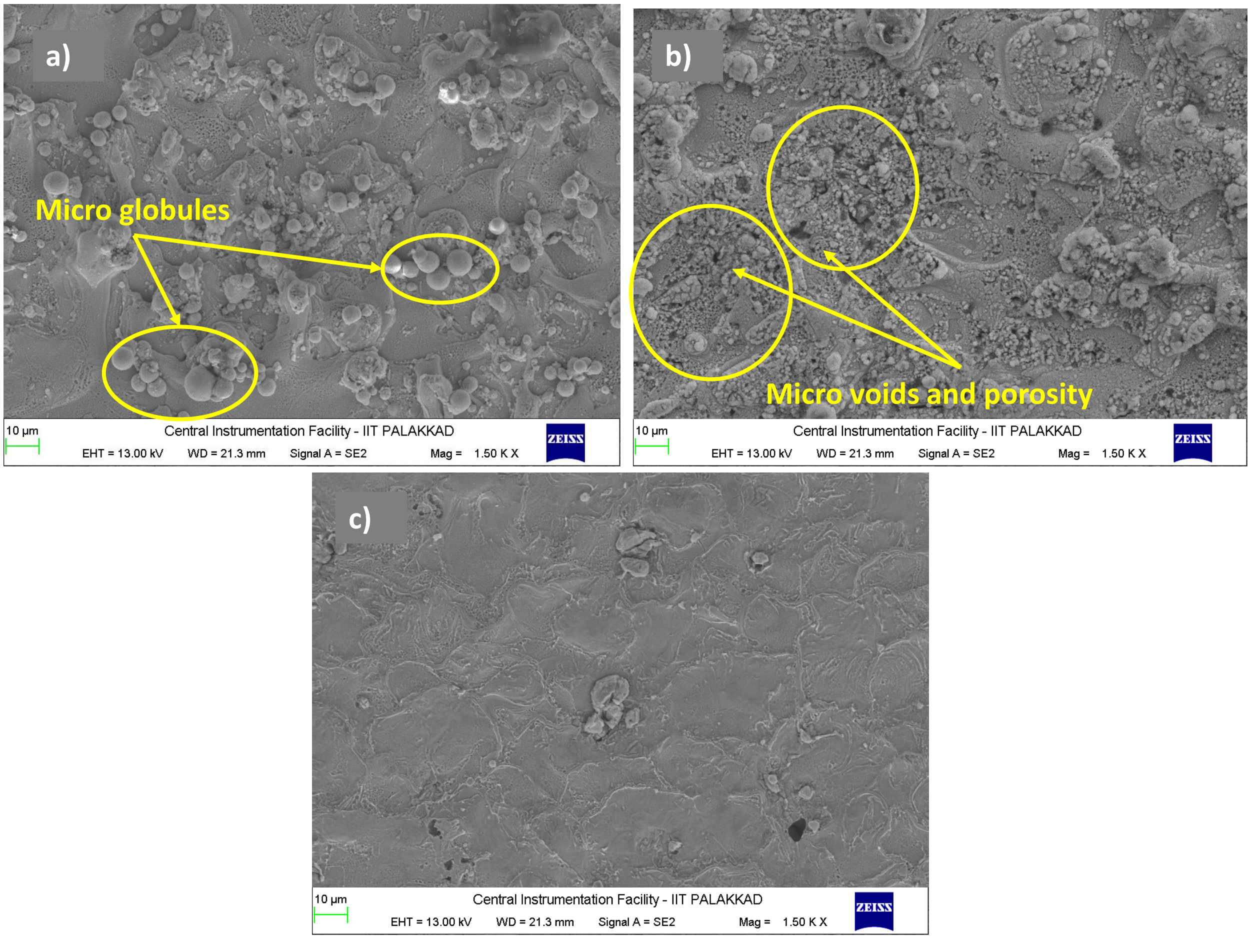

Fig. 6. SEM images of machined surface at discharge energy mode
(a) C1 (b) C3 (c) C5

3.5 Micro hardness tests

Micro hardness tests were conducted for the subsurface hardness study. The test results can be used to understand the thermal softening effects on the machined samples. The subsurface microhardness at various depts from the machined surface are shown in Fig. 7. The measurement is conducted on the polished cross-sectional surface underneath the curved machined surface as shown in the figure. Due to the very low C% (wt. 0.067%) of Inconel 718, the recast layer does not get harder than the bulk material [2]. Maximum recast layer thickness on WED machined surfaces will be less than 20 µm to 30 µm at the highest discharge energy settings. However, the heat affected zone (HAZ) extends to a much larger depth of 50 µm to 80 µm. Due to this reason, sub surface softening due to the thermal effects is observed till 50 µm in this case and then it steadies. The subsurface nearer to the machined surface is observed to have softened considerably. The effect is more pronounced in the case of C1 discharge energy settings whereas machined subsurface under C5 condition is observed to be the least affected. The reason for this is the higher discharge energy of sparks in the former case, which anneals and softens the immediate layers under the machined surface. Under C5 discharge energy mode, the discharge energy is comparatively smaller to thermally soften the surface and thus the effect is minimum. At C5, a mere 4% reduction in subsurface hardness compared to the bulk material was observed. This indicates near zero thermal effects on the machined specimen. The result is comparable with 7.2 % reduction reported by Sharma et al. [32] by the trim cut strategy. Figure shows the subsurface hardness profile when machined with hard zinc coated brass wire electrode. Similar trend was observed for all the wire electrode types.

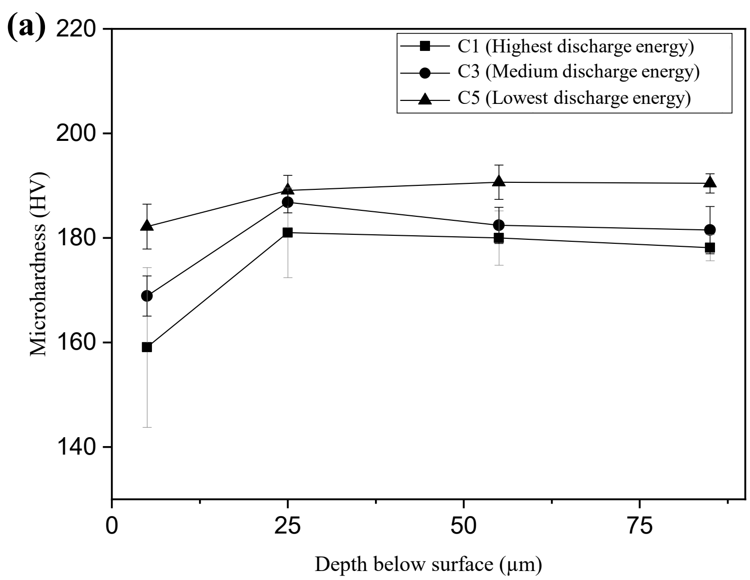

Fig. 7 (a) Subsurface microhardness profile

3.7 Metallurgical changes

Energy Dispersive Spectroscopy (EDS) analysis was performed to compare the elemental migration from the wire electrode to the machined surface. Elemental contamination is preferred to be minimal during any processing operation, since it alters the parent materials original properties. During WEDM operation with coated wires, migration of zinc from the wire material to the workpiece is considered as elemental contamination. This happens because, during the spark erosion, the material will be removed not just from the workpiece, but also from the wire electrode. Higher discharge energies remove more zinc from the wire surface coatings and this tends to migrate from wire to workpiece surface and get attached there. The weight percentage of zinc on the machined surface has reduced from 9.5 % to 1.7 % when the discharge energy mode is changed from C1 to C5 as shown in Fig. 8. Thus, the elemental contamination can be reduced to a greater extend by adjusting the spark discharge energy.

The effect of zinc contamination is less prominent in case of surfaces machined with uncoated brass electrode as seen in Fig. 9. During lowest discharge energy mode, the zinc element is hardly present on the surface. At highest energy settings, however, there were increased traces of both zinc and copper. It is therefore learnt that, for a minimum elemental contamination, usage of uncoated wire electrodes and lowest discharge energy settings is preferred.

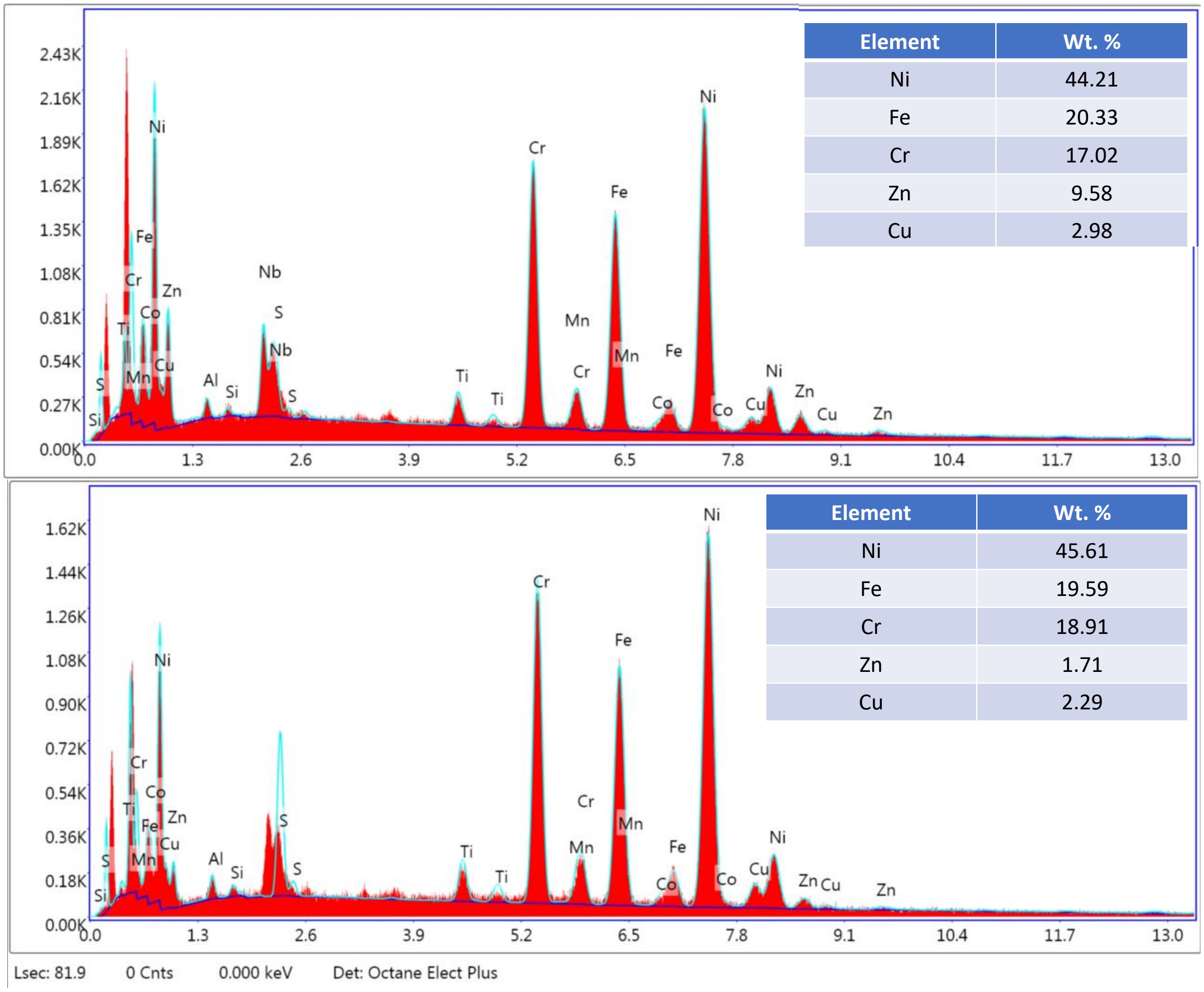

Fig. 8 EDS analysis of surface machined with hard zinc coated brass wire under

(a) Highest discharge energy, C1 (b) Lowest discharge energy, C5

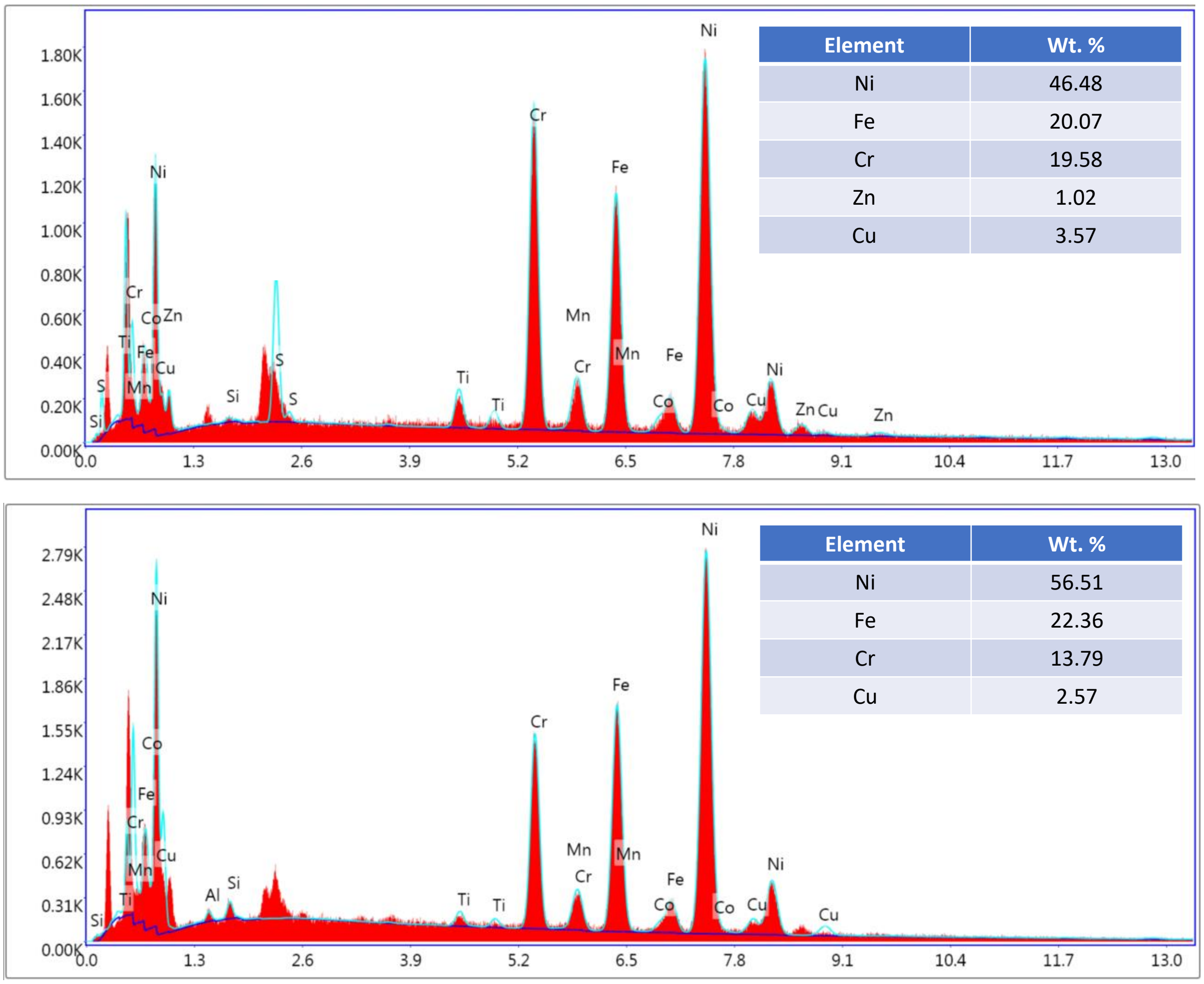

Fig. 9 EDS analysis of surface machined with hard uncoated brass wire under

(a) Highest discharge energy, C1 (b) Lowest discharge energy, C5

3.8 Microstructural analysis of wire surface

The wire wear patterns for coated and uncoated wire electrodes were analyzed using scanning electrode microscope. It is observed that, higher the discharge energy, greater is the wire wear for both types of wire electrodes. This effect is shown for the case of hard coated wires in Fig. 10. Similar surface features were observed for half hard-uncoated wire also. At highest discharge energy settings, C1, greater amount of wire coatings were removed. Extensive surface cracking has resulted in a highly uneven surface as shown in Fig. 10 (a). However, at discharge energy mode C5, wire coating was observed to be removed in the form of micro cracks when subjected to lower energy spark discharges. This effect is shown in Fig. 10 (b). The effect of surface cracking is exclusive to the wires coated with volatile metals like zinc. EDS analysis of the wire surfaces are given in Fig. 11. For the coated wires, it can be observed that the wt.% of zinc is reduced from 61.99 % to 53.86 % as the discharge energy mode goes from C5 to C1. This is because, greater amount of zinc coatings is removed at C1, exposing the underlying core brass material.

In the case of uncoated brass electrodes, the wire material erodes in the form of micro craters. The wire surface is observed to be devoid of any cracks as seen in the previous case. At highest discharge energy settings, C1, a deeper and wider crater or multiple overlapping craters were observed as in Fig. 12 (a). However, at C5, the wire surface is observed to be only slightly eroded with shallow intermittent craters as evident from Fig. 12 (b). The images shown are of hard uncoated brass wire. But it was observed that half hard-uncoated brass wire surface also revealed similar features.

The erosion patterns on the wire surface observed at C1, will result in extensive material removal and may eventually lead to wire breakages on further increasing the discharge energy. Compared to coated ones, the uncoated wire electrodes have lesser capacity to withstand higher energy discharges. This is because, the thermal shock experienced by the wire is higher due to absence of any coating. EDS analysis of the wire surfaces are given in Fig. 13. For uncoated material, EDS does not show compositional changes, since the composition of the brass wire remains the same even though more amount of wire wear is observed at C1.

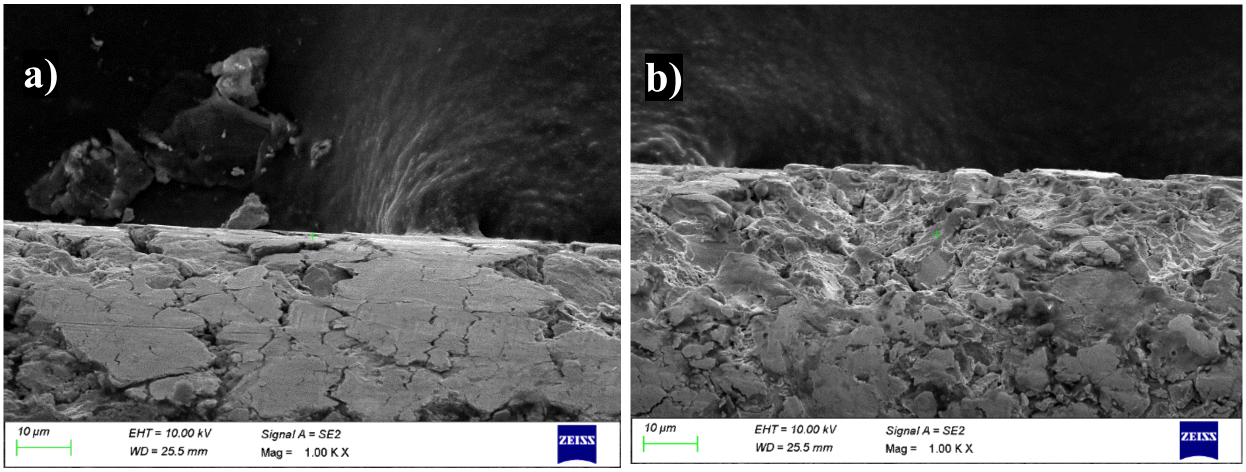

Fig. 10 SEM images of hard zinc coated brass wire surface at discharge energy mode (a) C1 (b) C5

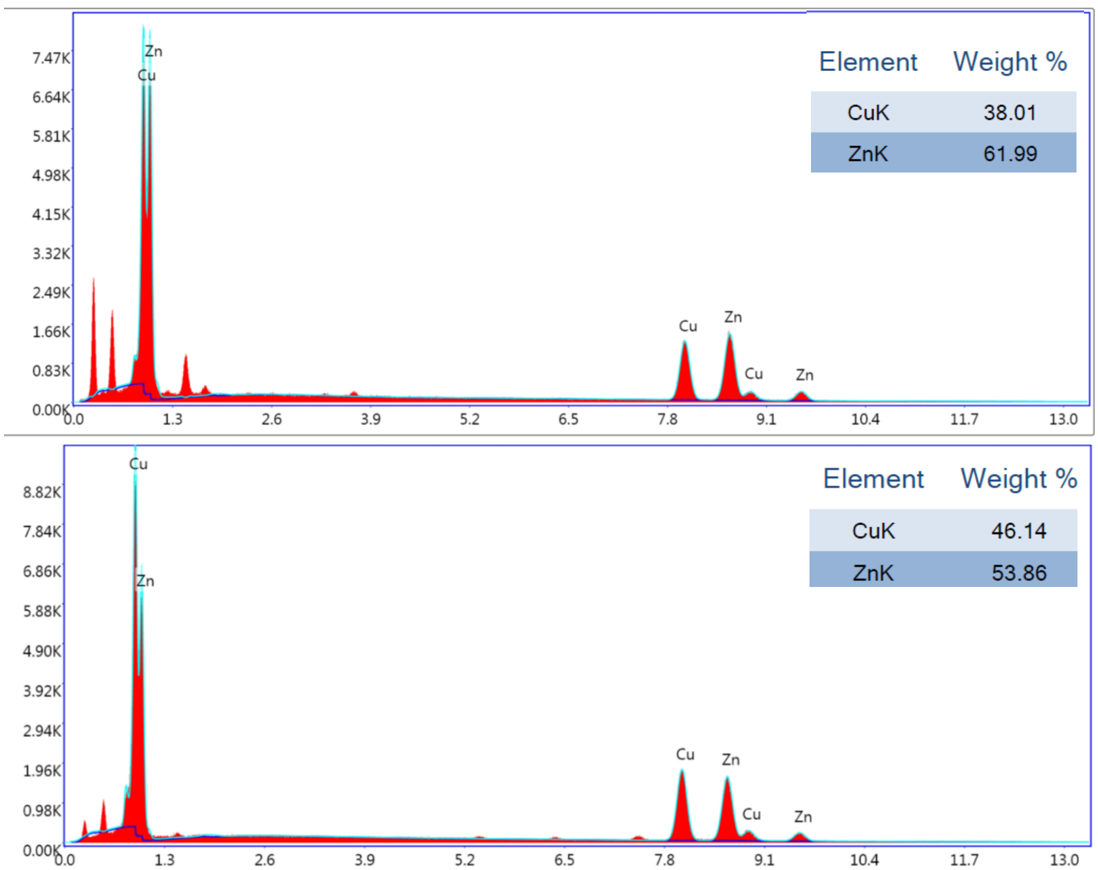

Fig. 11 EDS images of hard zinc coated brass wire surface at discharge energy mode (a) C1 (b) C5

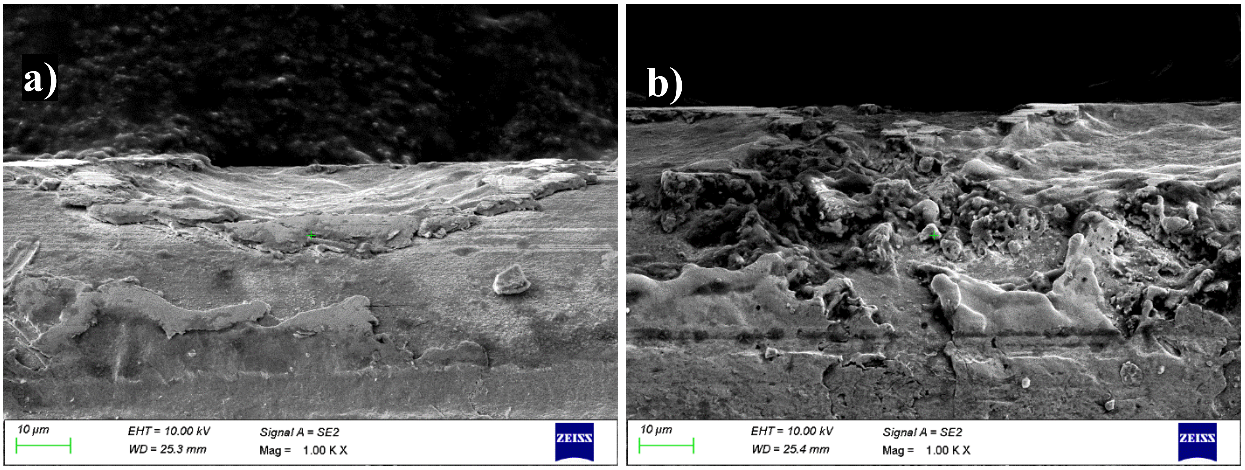

Fig. 12 SEM images of hard uncoated brass wire surface at discharge energy mode
(a) C1 (b) C5

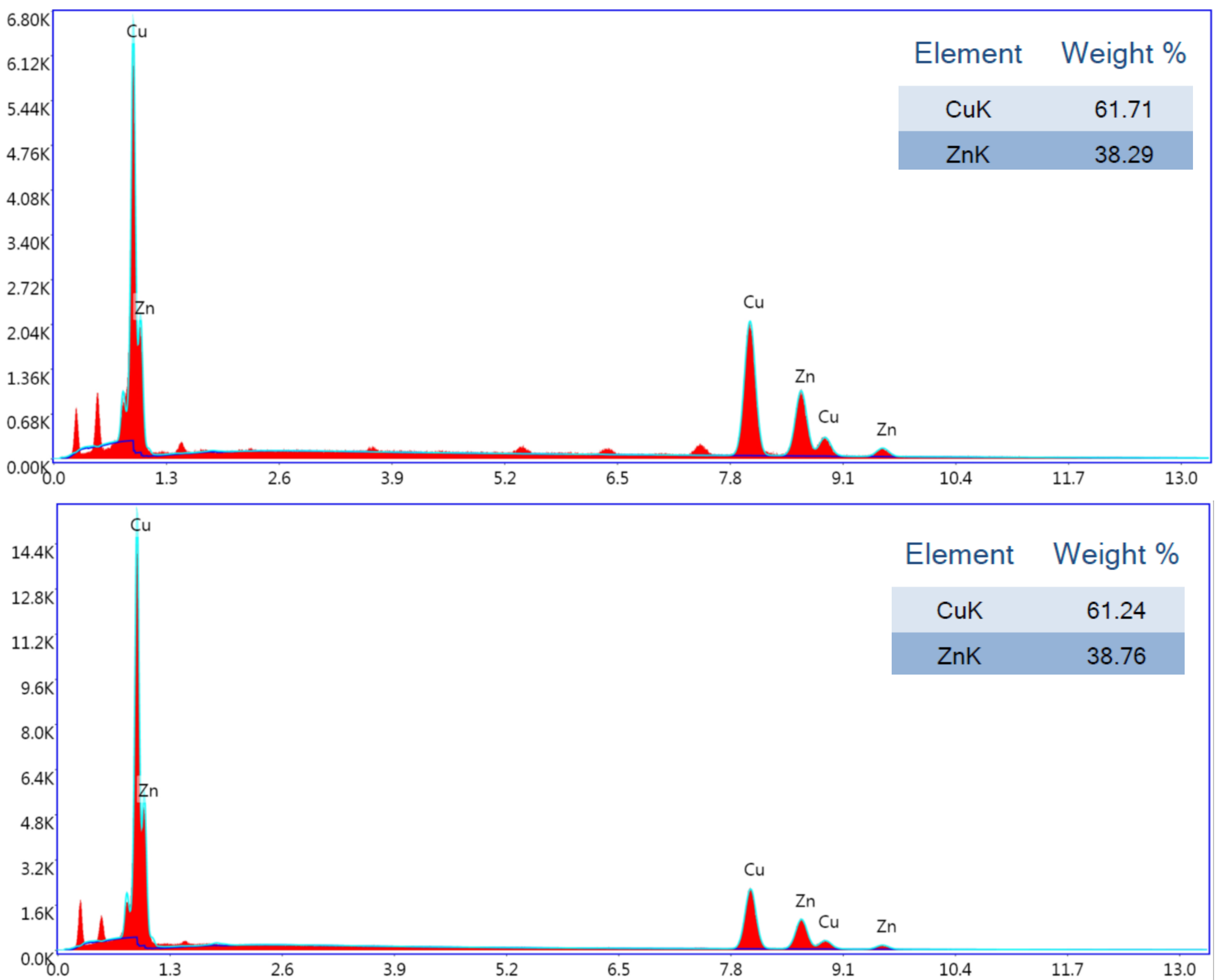

Fig. 13 EDS images of hard uncoated brass wire surface at discharge energy mode
(a) C1 (b) C5

3.9 Machining failure conditions

The two extreme scenarios which can occur outside the considered discharge energy range from C1 to C5 are wire breakages and spark absence. Both of those situations are discussed next.

3.9.1 Weak/insufficient sparks

The gap condition which is not suitable to sustain repetitive sparks will result in spark absence. This situation can occur when the discharge energy is deficient for material removal. Under such discharge energy settings, the machining did not happen due to absence of pulses on some instances or due to extremely weak pulses. Such pulses are called open circuit pulses where in the pulsed voltage input isn't high enough to ionize the dielectric fluid in the spark gap, to produce sufficiently strong discharges capable of machining the material.

3.9.2 Wire breakages

One of the most reported reasons for wire breakages are machining instabilities due to extremely high discharge energy. When the discharge energy is further increased than C1 condition, the wire material will be unable to withstand the energy and will eventually break. The discharge energy setting that caused wire rupture for coated and uncoated wires will be different. In case of uncoated electrode, as the discharge energy increases, deeper craters would form, leading to wire rupture. In the case of coated wire, extensive cracking of surface coatings would expose the bare brass core, leading to wire rupture. The coated wires will be able to withstand higher discharge energies before rupture.

The discharge characteristics were captured using voltage and current sensors and the resultant pulse cycle variations are shown in Fig. 14. At C5, the discharge spark frequency is less with desirable levels of pulse off and ignition delay time (Fig. 14 (a)). Further, the discharge frequency increases as the discharge energy goes up, as can be seen in Fig. 14 (b) and Fig. 14 (c). At C1, wire breakage conditions are indicated by series of short circuit sparks (Fig. 14 (d)). Similar pulse cycle trends are observed in the recent literature during condition monitoring of wire EDM [35-37].

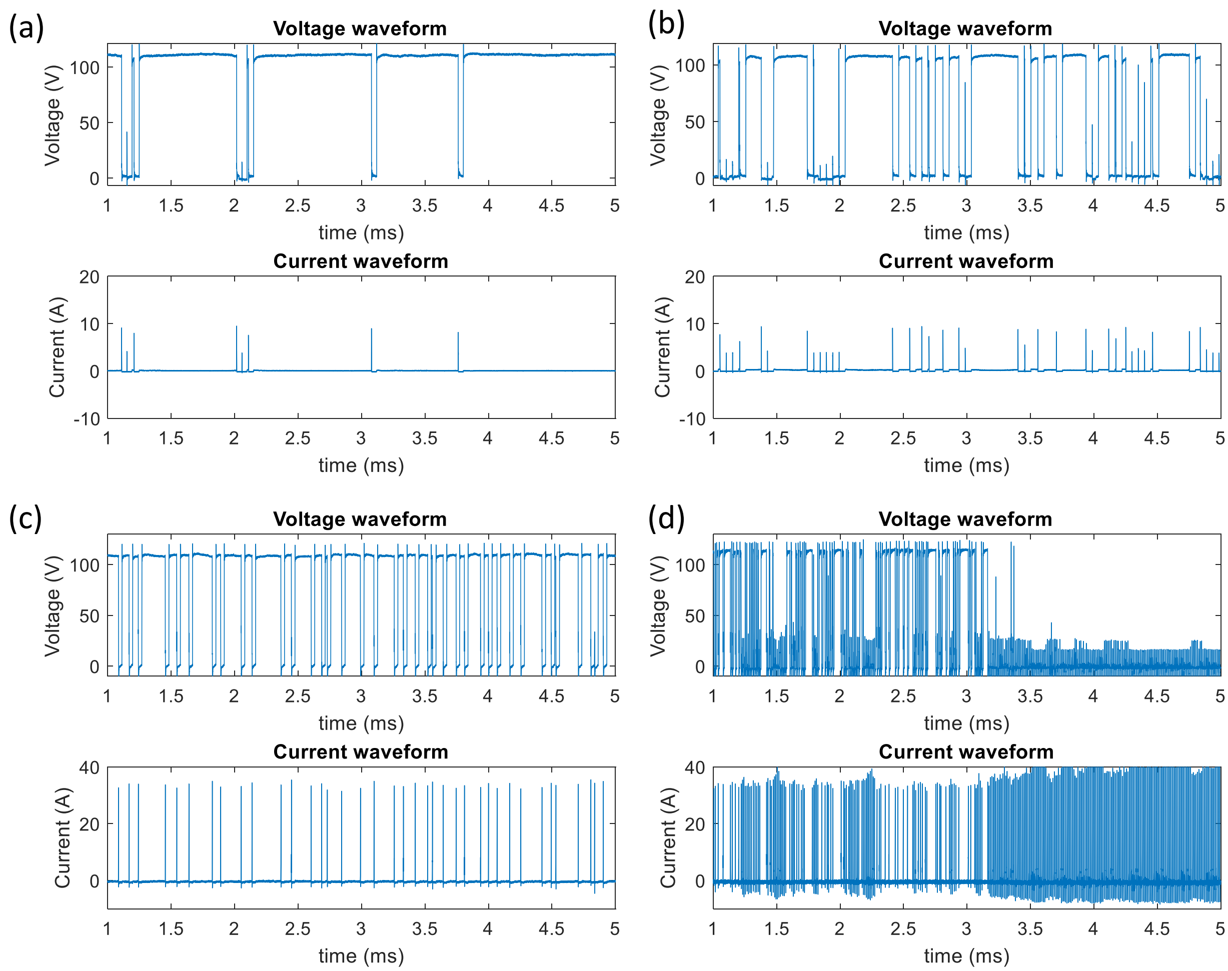

Fig. 14. Comparison of pulse discharge cycles at various discharge energy levels (a) C5 (b) C3 (c) C2 (d) C1

4. Conclusions

The study revealed that the wire material and discharge energy have a significant effect in determining the quality and productivity of machined components. The following are the conclusions from the current experimental analysis.

- Surface roughness and cutting speed were significantly influenced by discharge energy modes. Surface roughness was reduced by 46.9 % by changing the discharge energy mode from C1 (highest discharge energy mode) to C5 (lowest discharge energy mode). Coated wires were observed to cut 22 % faster than the uncoated wire electrodes.
- Both discharge energy and wire electrode types have significant effect on geometric accuracies. On bringing down the discharge energy from 0.01531 J to 0.01373 J, form errors like flatness error was reduced by 82.41 %, circularity error was reduced by 91.66 %, and cylindricity error was reduced 52.9 %.
- Hard wire electrodes can resist wire vibrations better and thus resulted in more geometrically accurate surfaces compared to half-hard wire electrodes.
- Subsurface microhardness analysis revealed a hardness drop closer to the machined surface compared to the bulk material. The thermal softening effect is more prominent at higher discharge energy modes due to annealing effects caused by higher energy sparks.
- The zinc and copper elemental contamination was minimal for uncoated wire electrodes under lowest discharge energy mode.
- Wire wear happens on coated and uncoated wire surfaces by the formation of micro cracks and micro craters respectively. In the case of coated wire electrodes, weight % of zinc on the wire electrode surface was reduced from 61.99 % during the lowest discharge energy settings to 53.86 % during the highest discharge energy settings due to the greater wire wear and subsequent removal of zinc coating.

Acknowledgement

The authors would like to thank the central instrumentation facility (CIF), IIT Palakkad, for providing the test facility and equipment.

Funding details: No funding was received to support this study.

Disclosure statement. Authors declare that there is no potential competing interest.

Data availability statement: All the data relevant for the study are given in the manuscript.

References

1. Reed RC. The Superalloys Fundamentals and Applications. Cambridge; 2006.
2. Li L, Guo YB, Wei XT, Li W. Surface integrity characteristics in wire-EDM of inconel 718 at different discharge energy. Procedia CIRP, 2013; 6: 220–5.
3. Ho KH, Newman ST, Rahimifard S, Allen RD. State of the art in wire electrical discharge machining (WEDM). Int J Mach Tools Manuf, 2004; 44: 1247–59.
4. Aggarwal V, Khangura SS, Garg RK. Parametric modeling and optimization for wire electrical discharge machining of Inconel 718 using response surface methodology. Int J Adv Manuf Technol, 2015; 79: 31–47.
5. Manjaiah M, Laubscher RF, Kumar A, Basavarajappa S. Parametric optimization of MRR and surface roughness in wire electro discharge machining (WEDM) of D2 steel using Taguchi-based utility approach. Int J Mech Mater Eng, 2016; 11: 7
6. Sarkar S, Mitra S, Bhattacharyya B. Parametric optimisation of wire electrical discharge machining of γ titanium aluminide alloy through an artificial neural network model. Int J Adv Manuf Technol, 2006; 27: 501–8.
7. Li L, Wei XT, Guo YB, Li W, Liu JF. Surface integrity of Inconel 718 by wire-EDM at different energy modes. J Mater Eng Perform, 2014; 23: 3051–3057.
8. Sharma P, Chakradhar D, Narendranath S. Effect of Wire Material on Productivity and Surface Integrity of WEDM-Processed Inconel 706 for Aircraft Application. J Mater Eng Perform, 2016; 25: 3672–3681.
9. Cabanes I, Portillo E, Marcos M, Sánchez JA. An industrial application for on-line detection of instability and wire breakage in wire EDM. J Mater Process Technol, 2008; 195: 101–109.
10. Kumar V, Jangra KK, Kumar V, Sharma N. WEDM of nickel based aerospace alloy: optimization of process parameters and modelling. Int J Interact Des Manuf, 2017; 11: 917–929.

11. Caggiano A, Teti R, Perez R, Xirouchakis P. Wire EDM monitoring for zero-defect manufacturing based on advanced sensor signal processing. Procedia CIRP, 2015; 33: 315–320.
12. Straka Ľ, Čorný I, Piteľ J. Prediction of the Geometrical Accuracy of the Machined Surface of the Tool Steel EN X30WCrV9-3 after Electrical Discharge Machining with CuZn37 Wire Electrode. Metals (Basel), 2017; 7:462.
13. H. Abyar, A. Abdullah, and A. Akbarzadeh Shafaroud, Theoretical and Experimental Analysis of Machining Errors on Small Arced Corners during WEDM Finishing Stages, Mach. Sci. Technol., Taylor & Francis, 2019; 23(5): 734–757, doi:10.1080/10910344.2019.1575410.
14. Prohaszka J, Mamalis AG, Vaxevanidis NM. The effect of electrode material on machinability in wire electro-discharge machining. J Mater Process Technol, 1997; 69: 233–237.
15. Islam MN, Rafai NH, Subramanian SS. Dimensional accuracy achievable in wire-cut electrical discharge machining. Lect Notes Electr Eng, 2011; 90 LNEE: 543–553.
16. Kumanan S, Nair A. Prediction of multi performance characteristics of wire EDM process using grey ANFIS. IOP Conf Ser Mater Sci Eng, 2017; 244.
17. Senkathir S, Aravind R, Samson RM, Raj ACA. Optimization of Machining Parameters of Inconel 718 by WEDM Using Response Surface Methodology. Adv Manuf Process, 2019; 383–392.
18. Pramanik A, Islam MN, Basak AK, Dong Y, Littlefair G, Prakash C. Optimizing dimensional accuracy of titanium alloy features produced by wire electrical discharge machining. Mater Manuf Process, 2019; 0: 1–8.
19. A. Ramamurthy, R. Sivaramakrishnan, T. Muthuramalingam, and S. Venugopal, Performance Analysis of Wire Electrodes on Machining Ti-6Al-4V Alloy Using Electrical Discharge Machining Process, Mach. Sci. Technol., 2015; 19(4): 577–592.
20. Reolon LW, Henning Laurindo CA, Torres RD, Amorim FL. WEDM performance and surface integrity of Inconel alloy IN718 with coated and uncoated wires. Int J Adv Manuf Technol, 2018.

21. Jadam T, Datta S, Masanta M. Study of surface integrity and machining performance during main/rough cut and trim/finish cut mode of WEDM on Ti–6Al–4V: effects of wire material. J Brazilian Soc Mech Sci Eng, 2019; 41: 151.
22. Klocke F, Welling D, Klink A, Veselovac D, Nöthe T, Perez R. Evaluation of advanced Wire-EDM capabilities for the manufacture of fir tree slots in inconel 718. Procedia CIRP, 2014; 14: 430–435.
23. I. Cabanes, E. Portillo, M. Marcos, and J.A. Sánchez, An Industrial Application for On-Line Detection of Instability and Wire Breakage in Wire EDM, J. Mater. Process. Technol., 2008; 195(1–3): 101–109.
24. F. Klocke, D. Welling, A. Klink, and R. Perez, Quality Assessment through In-Process Monitoring of Wire-EDM for Fir Tree Slot Production, New Prod. Technol. Aerosp. Ind. - 5th Mach. Innov. Conf. (MIC 2014)-Procedia CIRP, Elsevier B.V., 2014; 24(C): 97–102, doi:10.1016/j.procir.2014.07.136.
25. F. Klocke, D. Welling, J. Dieckmann, D. Veselovac, and R. Perez, Developments in Wire-EDM for the Manufacturing of Fir Tree Slots in Turbine Discs Made of Inconel 718, Key Eng. Mater., 2012; 504–506: 1177–1182, doi:10.4028/www.scientific.net/KEM.504-506.1177.
26. P.M. Abhilash and D. Chakradhar, Surface Integrity Comparison of Wire Electric Discharge Machined Inconel 718 Surfaces at Different Machining Stabilities, Procedia CIRP, Elsevier B.V., 2020; 87: 228–233, doi:10.1016/j.procir.2020.02.037.
27. M. Gostimirovic, P. Kovac, M. Sekulic, and B. Skoric, Influence of Discharge Energy on Machining Characteristics in EDM, J. Mech. Sci. Technol., 2012; 26(1):173–179.
28. C.-T. Lin, I.-F. Chung, and S.-Y. Huang, Improvement of Machining Accuracy by Fuzzy Logic at Corner Parts for Wire-EDM, Fuzzy Sets Syst., 2001; 122: 499–511, www.elsevier.com/locate/fss.
29. G. Zhang, H. Li, Z. Zhang, W. Ming, N. Wang, and Y. Huang, Vibration Modeling and Analysis of Wire during the WEDM Process, Mach. Sci. Technol., 2016; 20(2): 173–186.
30. K. Mouralova, T. Prokes, L. Benes, and P. Sliwkova, Analysis of Subsurface Defects Occurrence in Abrasion Resistant Creusabro Steel after WEDM Including the Study of Morphology and Surface Topography, Mach. Sci. Technol., Taylor & Francis, 2019; 0(0): 1–17, doi:10.1080/10910344.2019.1669166.

31. A. Kumar, V. Kumar, and J. Kumar, Microstructure Analysis and Material Transformation of Pure Titanium and Tool Wear Surface after Wire Electric Discharge Machining Process, Mach. Sci. Technol., 2014; 18(1): 47–77.
32. P. Sharma, A. Tripathy, and N. Sahoo, Evaluation of Surface Integrity of WEDM Processed Inconel 718 for Jet Engine Application, IOP Conf. Ser. Mater. Sci. Eng., 2018; 323(1).
33. Mandal, Kingshuk, Soumya Sarkar, Souren Mitra, and Dipankar Bose. 2020. "Surface Roughness and Surface Topography Evaluation of Al 6065-T6 Alloy Using Wire Electro-Discharge Machining (Wire EDM)." Advances in Materials and Processing Technologies 6 (1): 75–83. https://doi.org/10.1080/2374068X.2019.1704547.\
34. Manikyam, Sandeep, and P. Jamaleswara Kumar. 2021. "Experimental Investigation And Surface Quality Parameters Optimization In WEDM Machining Of D-Series Tool Steels." Advances in Materials and Processing Technologies 00 (00): 1–12. https://doi.org/10.1080/2374068X.2021.1946752.
35. Abhilash, P. M., and Dupadu Chakradhar. 2022. "Wire EDM Failure Prediction and Process Control Based on Sensor Fusion and Pulse Train Analysis." *International Journal of Advanced Manufacturing Technology* 118 (5–6): 1453–67. https://doi.org/10.1007/s00170-021-07974-8.
36. Abhilash, P M, and D Chakradhar. 2021. "Failure Detection and Control for Wire EDM Process Using Multiple Sensors." CIRP Journal of Manufacturing Science and Technology 33: 315–26. https://doi.org/10.1016/j.cirpj.2021.04.009.
37. Abhilash, P M, and D Chakradhar. 2020. "ANFIS Modelling of Mean Gap Voltage Variation to Predict Wire Breakages during Wire EDM of Inconel 718." CIRP Journal of Manufacturing Science and Technology 31: 153–64. https://doi.org/10.1016/j.cirpj.2020.10.007.